Reflection of barotropic vortices from a step-like topography (*)(**)

L. ZAVALA SANSÓN, G. J. F. VAN HEIJST and J. J. J. DOORSCHOOT
J. M. Burgers Centre, Department of Physics
Eindhoven University of Technology, Eindhoven, The Netherlands

(ricevuto il 18 Novembre 1998; approvato il 6 Maggio 1999)

Summary. — The motion of a barotropic vortex on a β-plane approaching a meridional, step-like topography is studied by means of laboratory experiments and numerical simulations. In the experimental arrangement, the north-south direction is defined by a uniform weakly sloping bottom in order to simulate the β-effect. The numerical simulations are performed by using a finite-differences code, which solves the barotropic non-divergent equation. Initially, the vortices are created at the eastern side of the step. Thus cyclonic (anticyclonic) vortices drift northwestward (southwestward) on the β-plane and eventually interact with the step. The study is focused on cases where $\omega_0 \Delta H > 0$, with ω_0 the initial vortex peak vorticity and ΔH the step height, defined positive for a step-down and negative for a step-up topography. In both situations (cyclones approaching a step-down and anticyclones approaching a step-up), the vortices are stopped from crossing the step. This dramatic effect on the vortex trajectory is due to the entrainment of fluid from the other side of the step. Due to potential vorticity conservation, these entrained fluid columns acquire oppositely signed vorticity (relative to the vortex) as they experience depth variations, and form together with the original vortex a dipolar structure that moves away from the step. This effect is referred to as "vortex reflection". The reflection effect is enhanced either by increasing the Rossby number or by decreasing the step height. In cases where $\omega_0 \Delta H < 0$, cyclonic (anticyclonic) vortices are able to cross a step-up (down).

PACS 92.10.Ei – Coriolis effects.
PACS 47.32 – Rotational flow and vorticity.
PACS 47.27 – Turbulent flows, convection, and heat transfer.
PACS 01.30.Cc – Conference proceedings.

1. – Introduction

In numerous geophysical situations, bottom topography plays a crucial role on the evolution of oceanic and atmospheric flows. In particular, the motivation for this study

(*) Paper presented at the International Workshop on "Vortex Dynamics in Geophysical Flows", Castro Marina (LE), Italy, 22-26 June 1998.
(**) The authors of this paper have agreed to not receive the proofs for correction.

comes from the motion of oceanic, mesoscale vortices related with the β-effect. During their drift, vortices may interact with topographic features (canyons, seamounts, escarpments, etc.) and modify their trajectory. This situation has a fundamental importance in physical oceanography, since vortices are able to transport significant amounts of heat and momentum along large distances. For instance, the Agulhas retroflection produces warm eddies, which drift northwestward along the South Atlantic. These rings are considered as an important source of heat, salt and energy from the Indian Ocean into the South Atlantic (see, *e.g.*, Byrne *et al.*, 1995). Thus the study of the Agulhas eddies is relevant in order to estimate the global heat and salinity budgets. Therefore, it is important to understand the role of bottom topography on their paths, as they drift through the South Atlantic (Kamenkovich *et al.*, 1996).

The aim of this paper is to study the interaction of barotropic vortices with a step-like bottom topography, by using experimental and numerical evidence, and to describe the basic physical mechanisms involved. This study is focused on barotropic vortices, in contrast with the baroclinic structure of oceanic vortices, because it is intended to gain a better understanding of the fundamental mechanisms of vortex-topography interaction, starting from the simpler barotropic situation. Besides, the barotropic case has proven to be a useful tool for the study of oceanic vortices (Dewar and Gailliard, 1994).

In order to study vortices under the influence of β, this effect is included in both the laboratory experiments and the numerical simulations. On a β-plane (in the northern hemisphere), it is well known that barotropic cyclones (anticyclones) drift in the northwestern (southwestern) direction (see, *e.g.*, Carnevale *et al.*, 1991). In the present paper the evolution of such vortices as they approach a step-like topography is discussed. Formulated more specifically, this study considers the case of a barotropic vortex with mean depth H_0 trying to cross a step, towards a region of depth $H_0 + \Delta H$, where ΔH is positive (negative) when the vortex approaches a step-down (up). The attention is mainly focused on the special case where $\omega_0 \Delta H > 0$, with ω_0 the vortex peak vorticity (positive for cyclones and negative for anticyclones); *i.e.* cyclonic vortices approaching a step-down and anticyclonic vortices approaching a step-up. These situations lead to "reflection" of the vortex from the step: the vortex-topography interaction prevents the vortex from crossing the step. The importance of the reflection on the vortex trajectory is evident when considering that it inhibits the westward translation. The observed interaction behaviour is in remarkable contrast to the other case, $\omega_0 \Delta H < 0$, which is briefly mentioned (for a more extensive description of this case, see, *e.g.*, Grimshaw *et al.*, 1994; Zavala Sansón and van Heijst, 1998).

Section **2** is devoted to the experimental results obtained in a rotating fluid tank, where the β-effect is simulated by an overall, weak slope (the so-called topographic β-plane). In that section, the reflection of a cyclonic vortex in the presence of a step-down topography ($\omega_0 > 0$, $\Delta H > 0$) is presented. The contrasting case of a cyclonic vortex crossing a step-up ($\omega_0 > 0$, $\Delta H < 0$) is also shown. Numerical results, obtained by solving the nondivergent barotropic equation (see, *e.g.*, Grimshaw *et al.*, 1994), are presented in sect. **3**. The good agreement between the experimental situation and the numerical simulations allows a physical interpretation of the reflection effect in terms of conservation of potential vorticity, and provides confidence in the validity of this approach. Because of experimental difficulties in producing stable anticyclones in the laboratory (Kloosterziel and van Heijst, 1991), the case of an anticyclonic vortex approaching a step-up ($\omega_0 < 0$, $\Delta H < 0$) has only been studied numerically. The

numerical simulations also reveal the importance of the Rossby number associated with the vortex and the step height. Finally, sect. 4 contains the discussions.

2. – Laboratory experiments

2·1. *Experimental arrangement.* – The laboratory experiments were performed in a rotating fluid tank. A schematic figure of the experimental set-up used for the experiments described in this paper is shown in fig. 1. The horizontal dimensions of the rectangular tank are 1 and 1.5 m, and the maximum water depth is 0.24 m. The tank rotates in the anticlockwise direction at a constant rate of $0.5\ s^{-1}$, which corresponds with a Coriolis parameter $f_0 = 1\ s^{-1}$. As has been mentioned in the previous section, the latitudinal variation in the Coriolis parameter f (the β-effect) is simulated in the laboratory by a uniformly sloping bottom in the rotating fluid tank. The sloping bottom has a maximum vertical size of 0.1 m, and the value for β is thus $0.42\ (m\,s)^{-1}$ (see, *e.g.*, van Heijst, 1994). The shallow region corresponds with "north". The importance of the β-effect on the flow evolution is measured by the nondimensional number

$$\beta' = \frac{\beta L}{f_0}\,, \tag{1}$$

where L is the typical length scale of the flow, in this case the size of the vortex. In the

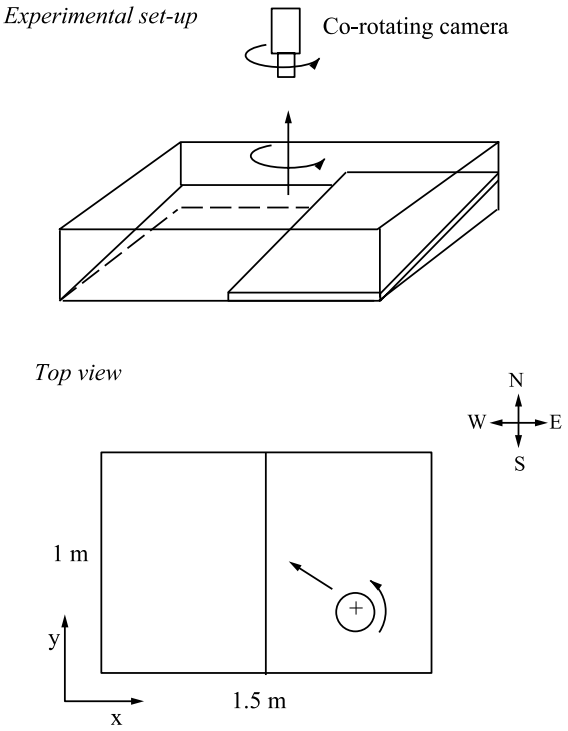

Fig. 1. – Schematic view of the experimental set-up. The lower graph shows a top view of the initial situation.

laboratory $L \sim 0.05$ m, and approximate values for β, L and f_0 in the ocean are 2×10^{-11} $(\mathrm{m\,s})^{-1}$, 10^5 m and $10^{-4}\,\mathrm{s}^{-1}$, respectively. For both cases this implies an approximate value of $\beta' \sim 0.02$, which indicates that the influences of the β-effect on a laboratory vortex and on a typical mesoscale, oceanic vortex are comparable.

On top of the topographic β-plane an additional topography is provided by a bottom plate which covers either the eastern or the western half of the tank (see fig. 1). Cyclonic vortices are created at the eastern side and drift northwestward, approaching the step-like topography. Hereafter, the difference in height between both regions, ΔH, is defined positive when the eastern side of the tank is shallow and the western side is deep; this is, when a vortex approaches a step-down topography.

In the laboratory, cyclonic vortices can be created in a rotating fluid by locally syphoning a fixed amount of fluid, during a certain period of time, through a thin perforated tube (for further details on this suction method see Carnevale *et al.*, 1991). For the flat-bottom case, typical radial distributions of the vorticity and azimuthal velocity are

$$\omega(r) = \omega_0 \exp\left[\frac{-r^2}{R^2}\right], \tag{2}$$

$$v(r) = \frac{R^2 \omega_0}{2r}\left(1 - \exp\left[\frac{-r^2}{R^2}\right]\right), \tag{3}$$

where ω_0 is the peak vorticity, R the horizontal length scale, and r the distance to the centre of the vortex. Typical vortex parameters are $\omega_0 \sim 1$ to $3\,\mathrm{s}^{-1}$ and $R \sim 0.03$ to 0.05 m. Thus the Rossby number, defined as ω_0/f_0, is initially O(1). These so-called "sink vortices" have a single-signed vorticity. Unfortunately, it is extremely difficult to obtain stable anticyclonic structures in the laboratory (see Kloosterziel and van Heijst, 1991). For this reason, the reflection of an anticyclonic vortex has been studied only by numerical simulations.

In the laboratory experiments the flow evolution is recorded by a co-rotating camera mounted at some distance above the rotating tank. The flow has been visualised in two ways: by adding fluorescent dye to the water, or by tracer particles floating on the surface. The latter method visualises the flow in the entire tank and the obtained video images can be processed with the digital image processing package DigImage (Dalziel, 1992). With this technique, the positions and velocities of large numbers of tracers are determined, which are interpolated onto a rectangular grid in order to calculate the velocity, vorticity and stream function fields.

2·2. *Reflection of a cyclonic vortex.* – Figure 2 shows a sequence of plan view photographs, illustrating the evolution of the dye distribution in an experiment on a sink vortex approaching a step-down topography ($\omega_0 > 0$, $\Delta H > 0$). The coordinates for the initial position of the vortex centre were $(x_0, y_0) = (1.10\ \mathrm{m}, 0.25\ \mathrm{m})$, with the origin (0, 0) taken at the most south-western point of the tank. The step was located at $x_s = 0.75$ m, and the difference in height between western and eastern regions was $\Delta H = 0.04$ m. As has been explained in the previous subsection, the vortex will start to drift in northwestern direction, thus approaching the topographic step. However, the vortex is not able to cross into the deeper part of the tank, but is actually reflected from the step ($t = 60$–120 s).

To understand the reflection effect, fig. 3 shows the streamlines obtained in an experiment similar to that shown in fig. 2. When the vortex starts the northwestward

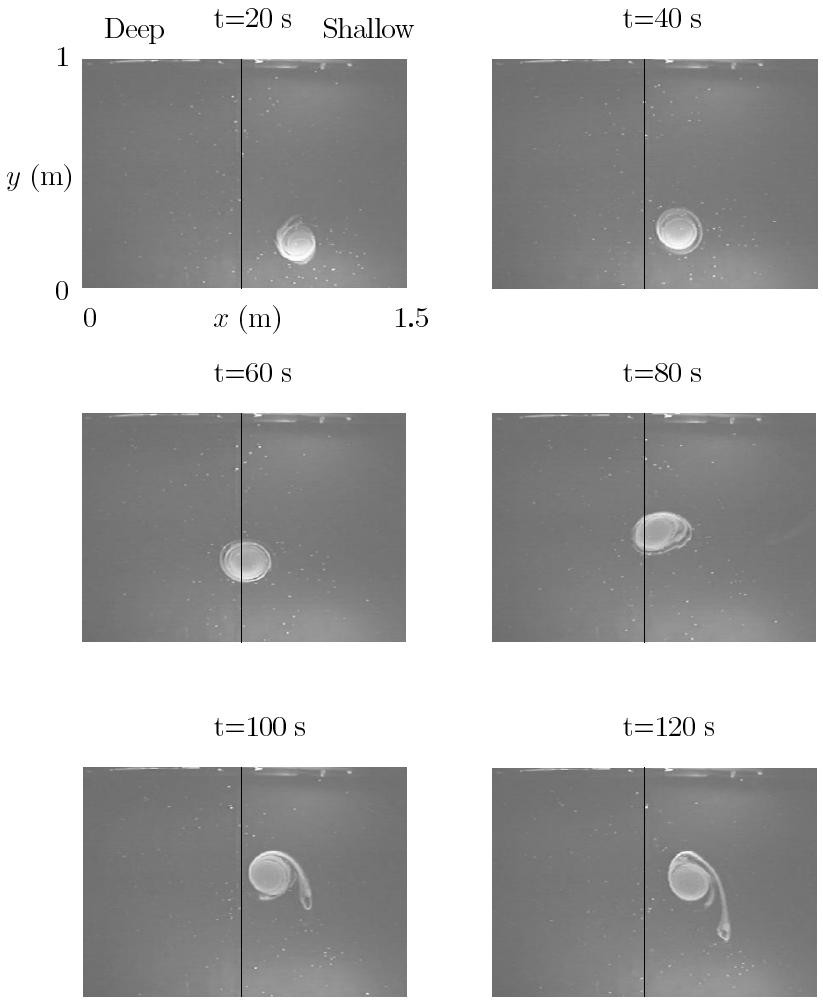

Fig. 2. – Top view photographs showing the reflection of a cyclonic vortex from a step-down topography. The vortex is visualised with bright dye. The step is indicated with a vertical line at $x = 0.75$ m.

drift, it radiates Rossby waves due to the β-effect. This is clearly visible in the first picture ($t = 20$ s), which shows an anticyclonic circulation cell at the northeastern side of the vortex. Once the vortex has reached the step, it drags fluid across the step, on the southern side of its core. As these fluid parcels are advected from the deep to the shallow side of the step, they gain negative vorticity, due to potential vorticity conservation. At the same time, the large negative cell that was generated has moved in south-western direction on the eastern side of the vortex. This Rossby cell reaches the southern side of the cyclone simultaneously with the formation of negative vorticity due to the step, and these two effects seem to amplify each other ($t = 60$ s). As a result, a dipolar structure arises, formed by the cyclone and the induced negative cell. The self-advecting mechanism of this dipolar structure pushes the cyclone away from the

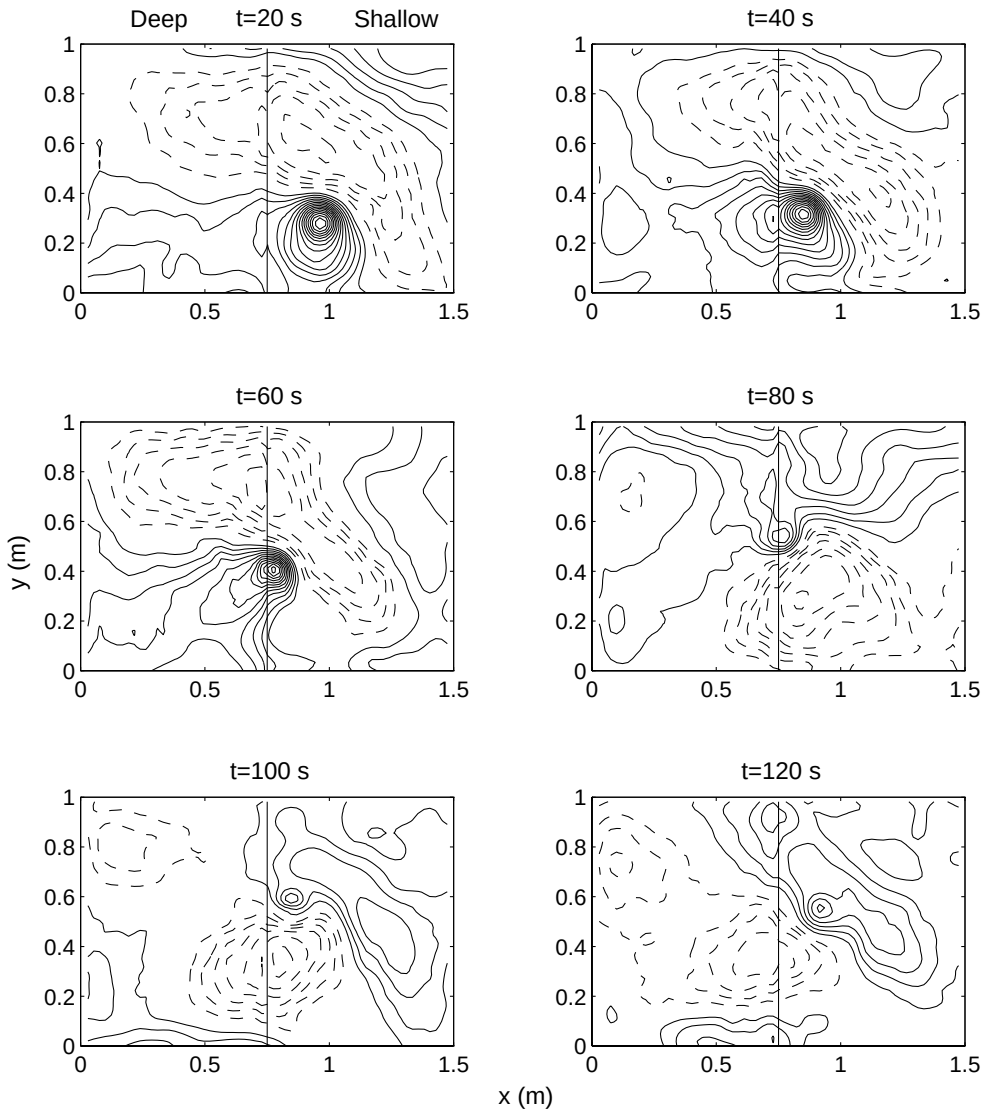

Fig. 3. – Stream function contours (the interval $\Delta\psi$ is $3 \times 10^{-5}\,\mathrm{m^3\,s^{-1}}$) of a case similar to that in fig. 2. The initial vortex parameters are approximately: $(x_0,\, y_0) = (1.10\,\mathrm{m},\, 0.25\,\mathrm{m})$, $R \sim 0.04$ m and $\omega_0 \sim 2.5\,\mathrm{s^{-1}}$.

step, and prevents it from crossing to the deep part of the tank. It is this generation of a cell of oppositely signed vorticity pairing with the original vortex—thus leading to the formation of a dipolar structure–that forms the basic mechanism of the reflection.

In order to examine the vortex behaviour in more detail, fig. 4a shows the vortex position every 10 seconds during the experiment shown in fig. 3. After the vortex has been reflected from the step, it seems to recover its original tendency and to drift in northwestern direction again. The experiment ended when the cyclone had dissipated by lateral viscous effects and bottom friction.

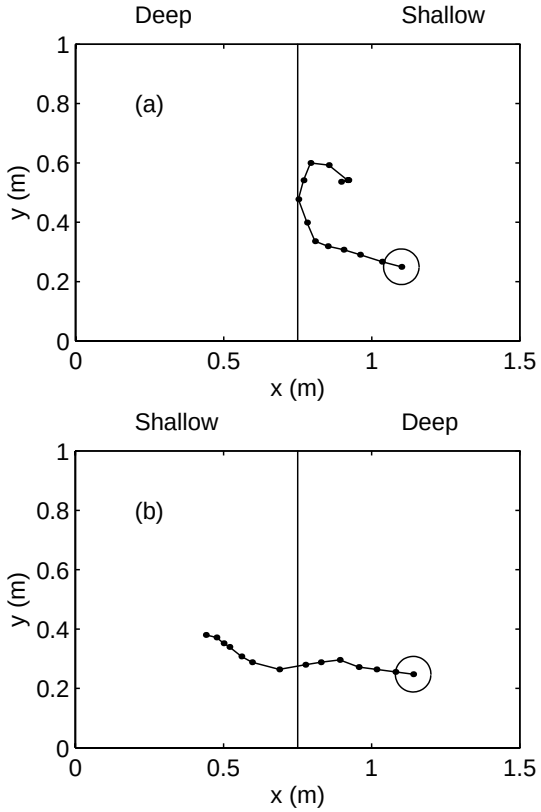

Fig. 4. – Experimental trajectories of cyclonic vortices meeting (a) a step-down and (b) a step-up.

The case of a cyclonic vortex approaching a step-up topography ($\omega_0 > 0$, $\Delta H < 0$) is completely different. Figure 5 contains a sequence of photographs showing a cyclonic vortex approaching and crossing a step-up topography ($\Delta H = -0.04$ m). The vortex (and its initial position) is similar to that in fig. 2. The main difference is that for the step-up case the vortex crosses the topography, approximately following the original northwestward drift. Figure 4b also shows the vortex trajectory, which has a small deviation to the southwest when crossing the step, and afterwards recovers the northwestern direction. Figure 6 shows the stream function field from an experiment similar to that in fig. 5. Following the previous arguments for the step-down case, the fluid dragged across the step at the southern side of the vortex core now does not form a negative circulation cell, since that fluid is crossing from shallow into deep waters. Thus the dipolar structure is not formed as in the step-down case, and the vortex crosses the step. The negative Rossby cell is not able to stop the vortex either.

3. – Numerical simulations

In addition to the laboratory experiments the evolution of vortices interacting with step-like topography variations has also been studied by numerical simulations based

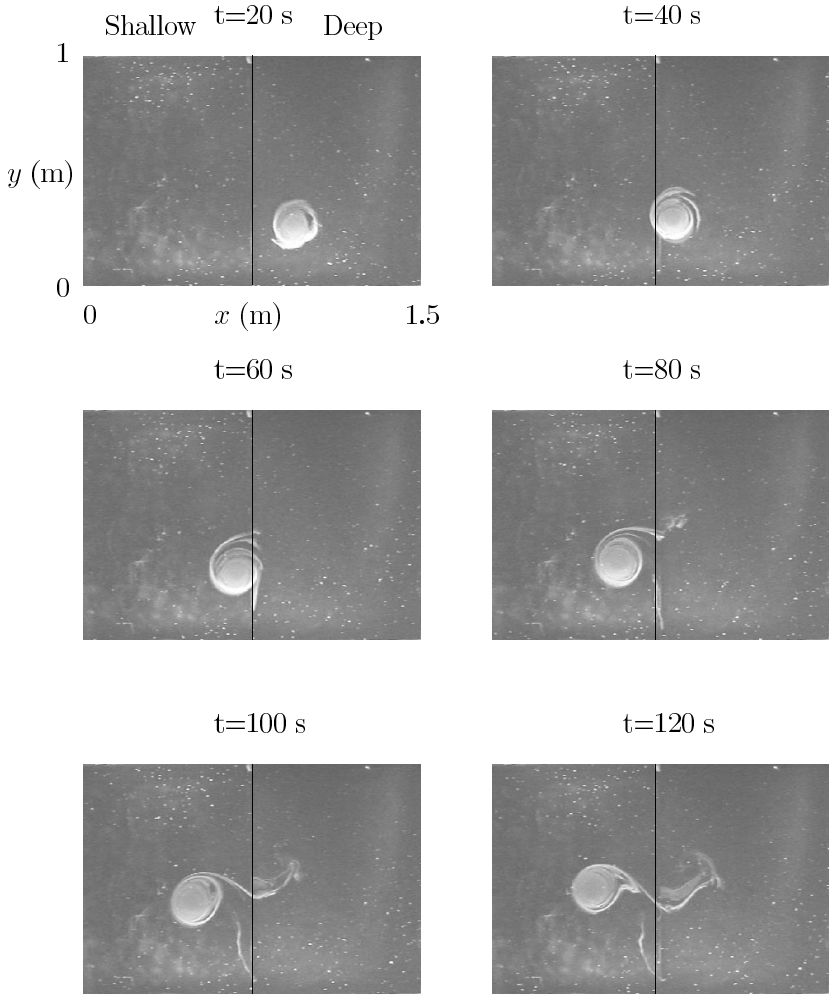

Fig. 5. – Top view photographs showing a cyclonic vortex crossing over a step-up topography. The vortex is visualised with bright dye. The step is indicated with a vertical line at $x = 0.75$ m.

on the barotropic nondivergent equation (see, *e.g.*, Grimshaw *et al.*, 1994), which is solved by using a finite-differences code. The aim of performing numerical simulations is to show that the observed vortex behaviour in the laboratory experiments can be explained by means of a (relatively) simple barotropic model.

3·1. *The model.* – In order to simulate the behaviour of a homogeneous fluid layer over topography numerically, it is assumed that the flow is governed by the barotropic nondivergent vorticity equation. In this model, the free-surface effects in the continuity equation are neglected. Thus, stretching-squeezing effects on fluid columns are due only to depth variations associated with the bottom topography. Vertical integration of the continuity equation results in $\partial(hu)/\partial x + \partial(hv)/\partial y = 0$, where u and v are the horizontal velocity components and $h(x, y)$ is the fluid depth, depending on

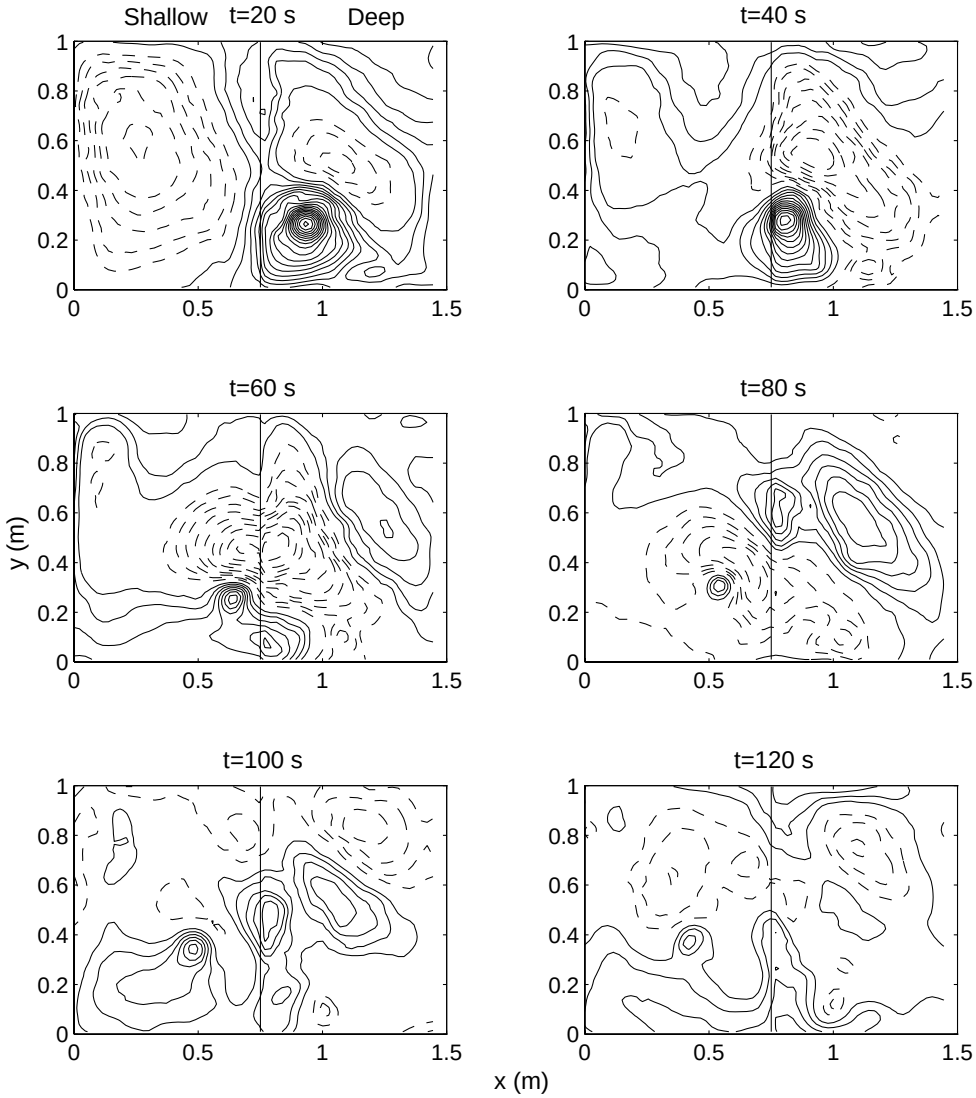

Fig. 6. – Stream function contours (the interval $\Delta\psi$ is $3 \times 10^{-5}\,\mathrm{m^3\,s^{-1}}$) of a similar case to that in fig. 5. The initial vortex parameters are approximately: $(x_0,\, y_0) = (1.10\ \mathrm{m},\, 0.25\ \mathrm{m})$, $R \sim 0.04$ m and $\omega_0 \sim 2.5\ \mathrm{s^{-1}}$.

the topography. Thus, a stream function ψ can be defined by

$$hu = \frac{\partial \psi}{\partial y}\,, \qquad hv = -\,\frac{\partial \psi}{\partial x}\,.$$

In this model the flow is governed by an evolution equation for the relative vorticity ω

$$\frac{\partial \omega}{\partial t} + J\left(\frac{\omega + f_0 + \beta y}{h}\,,\, \psi\right) = \nu \nabla^2 \omega\,, \tag{4}$$

where the vorticity is related to the stream function through

$$\omega = -\frac{1}{h}\nabla^2\psi + \frac{1}{h^2}\nabla h\cdot\nabla\psi\ . \tag{5}$$

The system (4) and (5) is solved with a finite-differences code. Initially, the code was developed by Orlandi and Verzicco (see Orlandi, 1990) for purely two-dimensional flows, and later extended by van Geffen (1998) in order to include rotational effects. In this paper, topographic effects are included in the code by means of the barotropic nondivergent model.

The numerical simulations were performed for flow on a real β-plane instead of the topographic β-plane used in the laboratory experiments. The value for β was $0.42\ (\mathrm{m\,s})^{-1}$, similar to the experimental β, and ν was taken to be $10^{-6}\ \mathrm{m^2\,s^{-1}}$. The mean depth was $H_0 = 0.20$ m. A feature which is not included in the numerical code is the presence of the Ekman layer on the bottom. This layer is partially responsible for the spinning down of the vortex. The experimental domain was discretised by 129×129 grid points. The step-like topography in the simulations is actually a very narrow slope (whose width is the distance between two grid points in the x-direction, which is much smaller than the vortex size), since the topography gradient $\partial h/\partial x$ cannot be infinite. Additional simulations using less narrow slopes (but always smaller than the vortex size) or doubling the grid resolution showed very similar results. No-slip boundary conditions were imposed in order to simulate the rotating tank experiments. The initial vorticity and velocity distributions were given by eqs. (2) and (3), where the vortex parameters, ω_0 and R, were similar to those in the experiments (taking $\omega_0 < 0$ for anticyclonic vortices).

3·2. *Cyclonic vortex approaching a step-down.* – Figures 7a and b show stream function and vorticity plots of numerical simulations of a cyclonic vortex approaching a step-down topography ($\omega_0 > 0$, $\Delta H > 0$), which can be compared with fig. 3. The vortex parameters and its initial position are $\omega_0 = 2.5\ \mathrm{s^{-1}}$, $R = 0.04$ m and $(x_0, y_0) = (1.10\ \mathrm{m}, 0.25\ \mathrm{m})$, respectively. The step is $\Delta H = 0.04$ m. When the vortex reaches the step, a negative circulation cell is formed at the southern part of the cyclone (t=60 s), which stops its northwestern drift. This entrainment of fluid from the western into the eastern side of the domain is clearly visible in the numerically calculated transport of a distribution of passive tracers, as shown in fig. 7c. At $t = 0$ s, a rectangular patch of passive tracers (0.60 m long, 0.20 m wide and centred at (0.65 m, 0.50 m)) was meridionally placed at the deep part of the tank, next to the step. As the vortex reaches the step, some tracers are advected into the shallow part of the tank creating the negative circulation cell, which pairs with the cyclone and stops its northwestern drift. The calculated vortex trajectory is also shown in these graphs. This simulation shows that the basic mechanism for the vortex reflection is the squeezing of fluid columns as they are advected by the vortex from deep into shallow waters.

The generation of Rossby waves is clearly visible from the beginning of the simulation. However, the shape and evolution of these large scale cells is somewhat different from those in the experiments. In the laboratory, it takes a few seconds to create the vortex by syphoning water out of the tank; during this time the size, strength and position of the vortex have already been affected by the topographic β-plane. Therefore the numerical initial condition is not exactly that of the experiment, so that some differences in the flow evolutions arise. The general behaviour, in particular the vortex reflection, is qualitatively similar, however.

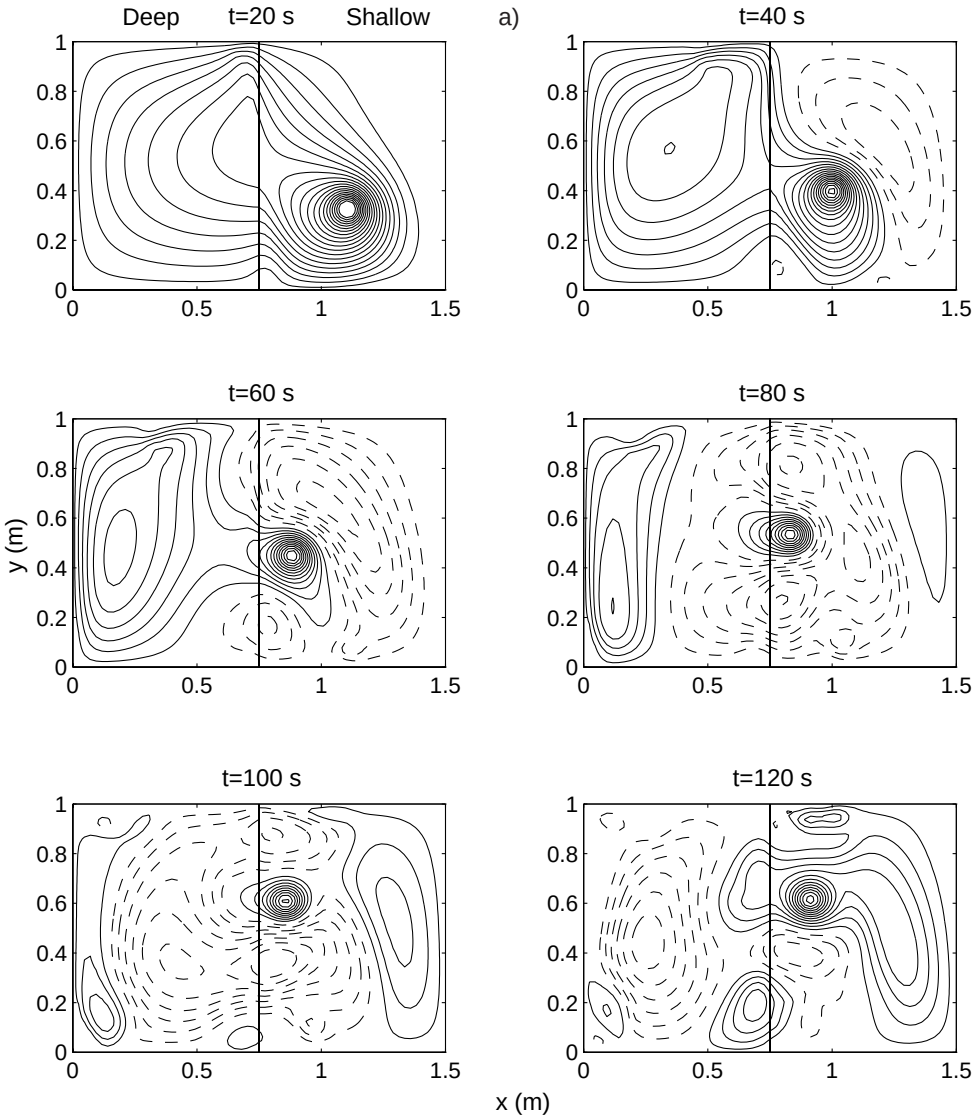

Fig. 7. – Numerical simulation of a cyclonic vortex approaching a step-down; the vortex parameters are the same as in the experiment shown in fig. 3. a) Stream function contours (the interval $\Delta\psi$ is $3 \times 10^{-5}\,\mathrm{m^3\,s^{-1}}$).

3·3. *Anticyclonic vortex approaching a step-up.* – Consider now an anticyclonic vortex approaching a step-up topography ($\omega_0 < 0$, $\Delta H < 0$). In this case, one observes again the reflection of the vortex from the step, *i.e.* an anticyclone is not able to cross a step-up topography. Figures 8a and b show the evolution of the corresponding stream function and vorticity fields in a numerical simulation initiated with the same vortex parameters as in fig. 7, but now setting $-\omega_0$. The initial position was $(x_0, y_0) = (1.10\,\mathrm{m},\ 0.75\,\mathrm{m})$. From these figures it is clear that the same mechanism stops the

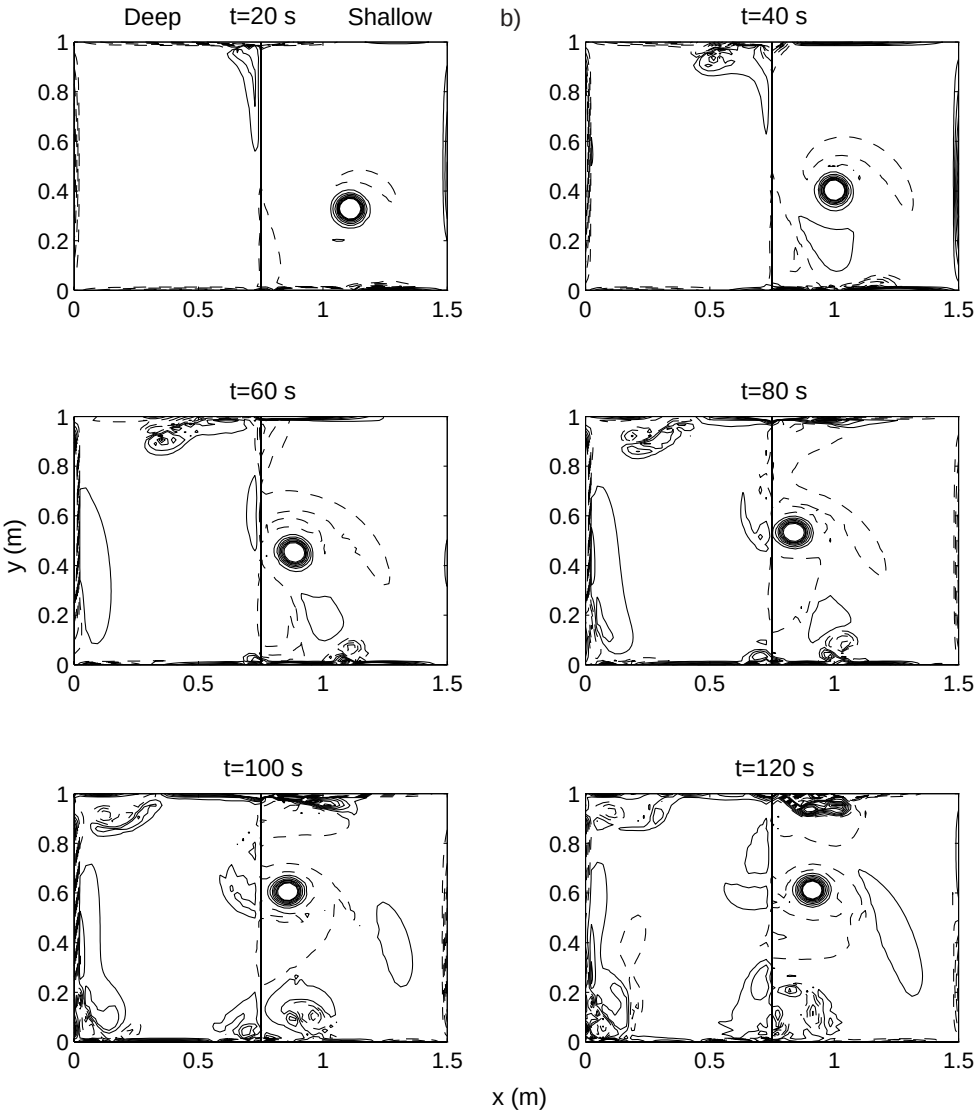

Fig. 7. – (*Continued.*) b) Vorticity contours (the interval $\Delta\omega$ is 0.1 s^{-1}).

anticyclone from crossing the step: a positive circulation cell is created at the northern part of the vortex ($t = 60$ s) when the anticyclone advects fluid from shallow into deep waters. This cell pairs with the original vortex and stops its southwestward motion. Figure 8c contains a sequence of plots similar to that in fig. 7c, showing the evolution of a patch of passive tracers initially placed at the shallow side of the tank, as well as the calculated vortex trajectory. When some fluid is advected across the step into the deeper part of the domain, a positive circulation cell is formed and the vortex migration is stopped.

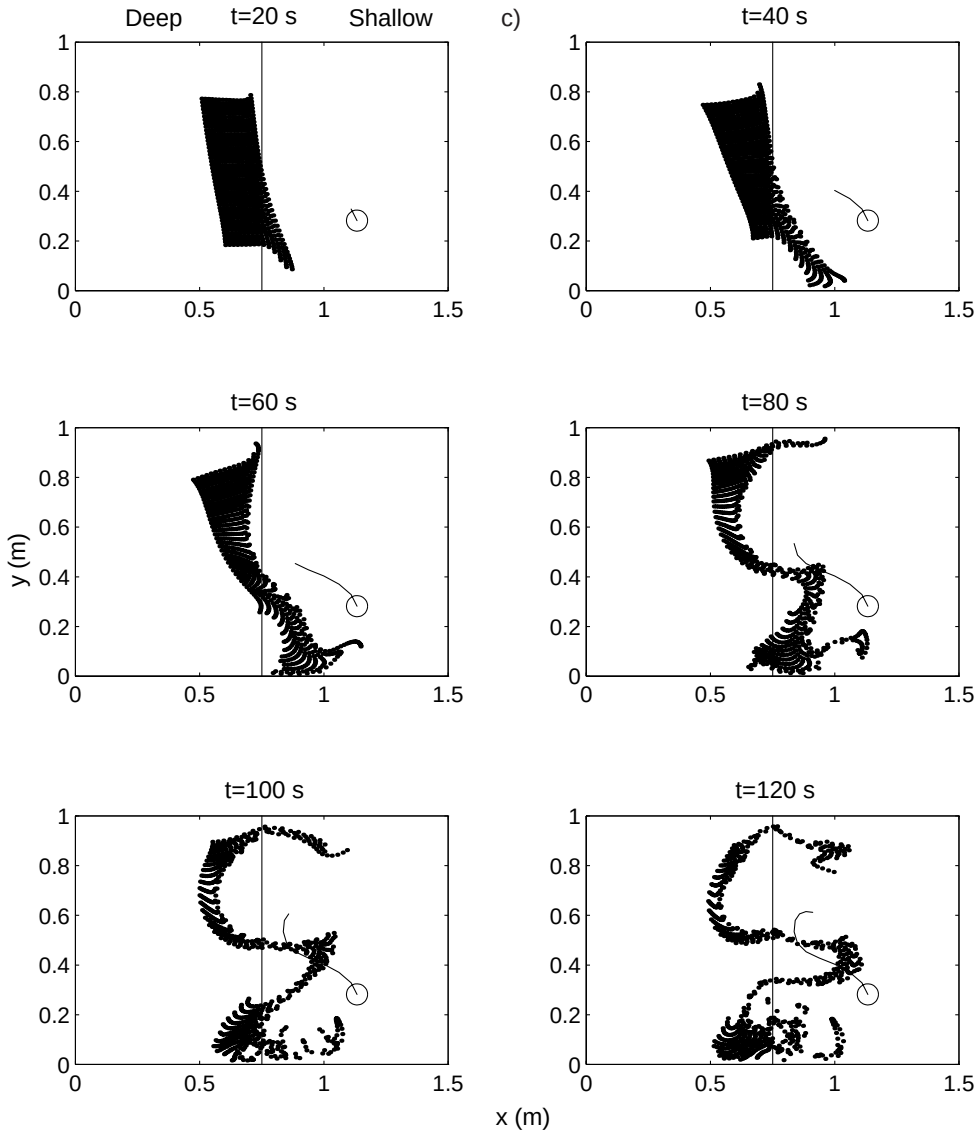

Fig. 7. – (*Continued.*) c) Evolution of passive tracers along the step. The initial vortex size and the vortex trajectory are indicated. The simulation is on a pure β-plane, *i.e.* only the step-like topography is included.

3·4. *Variation of step and vortex properties.* – Up to here, the reflection effect has been demonstrated for cases where $\omega_0 \Delta H > 0$. Obviously, in the limit $\Delta H \to 0$ this effect (or any topographic influence) is no longer present, and the case of a vortex moving on a β-plane is recovered. What are the critical step height and vortex parameters still able to produce the vortex reflection? Once the main physical mechanisms involved in the reflection are known, it is possible to predict these values to some approximation. Consider first the case of a cyclonic vortex approaching a

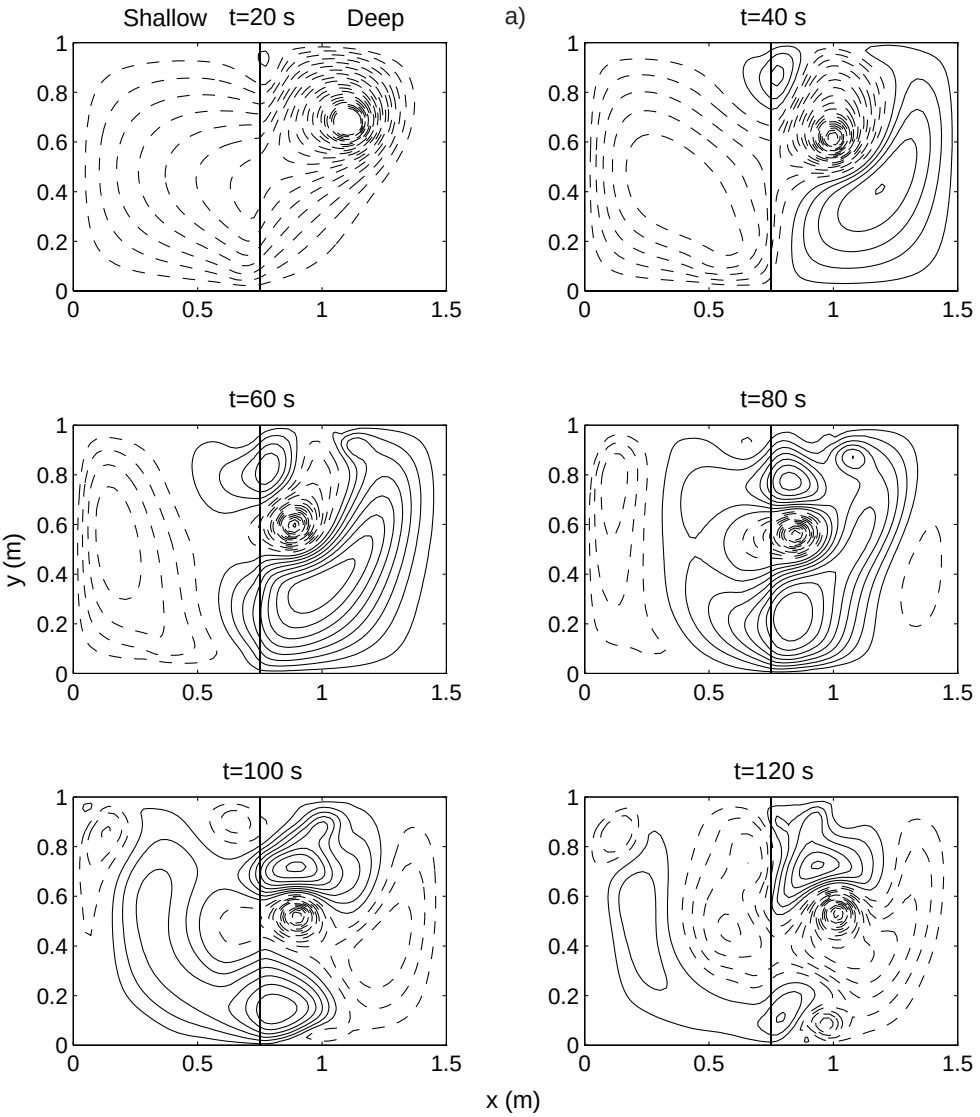

Fig. 8. – Numerical simulation of an anticyclonic vortex approaching a step-up; the vortex parameters are those in fig. 3 but now using $-\omega_0$ and $(x_0, y_0) = (1.10\,\mathrm{m},\ 0.75\,\mathrm{m})$. a) As in fig. 7a).

step-down ($\omega_0 > 0$, $\Delta H > 0$). As has been explained, the vortex reflection mechanism consists in the formation of a dipolar structure created from the vortex-step interaction, which moves away from the step. The positive half (ω^+) of this dipole is the vortex itself, while the negative half (ω^-) is formed with entrained fluid from the deep side of the step. The peak vorticities of both halves are

$$\omega^+ = \omega_0, \tag{6}$$

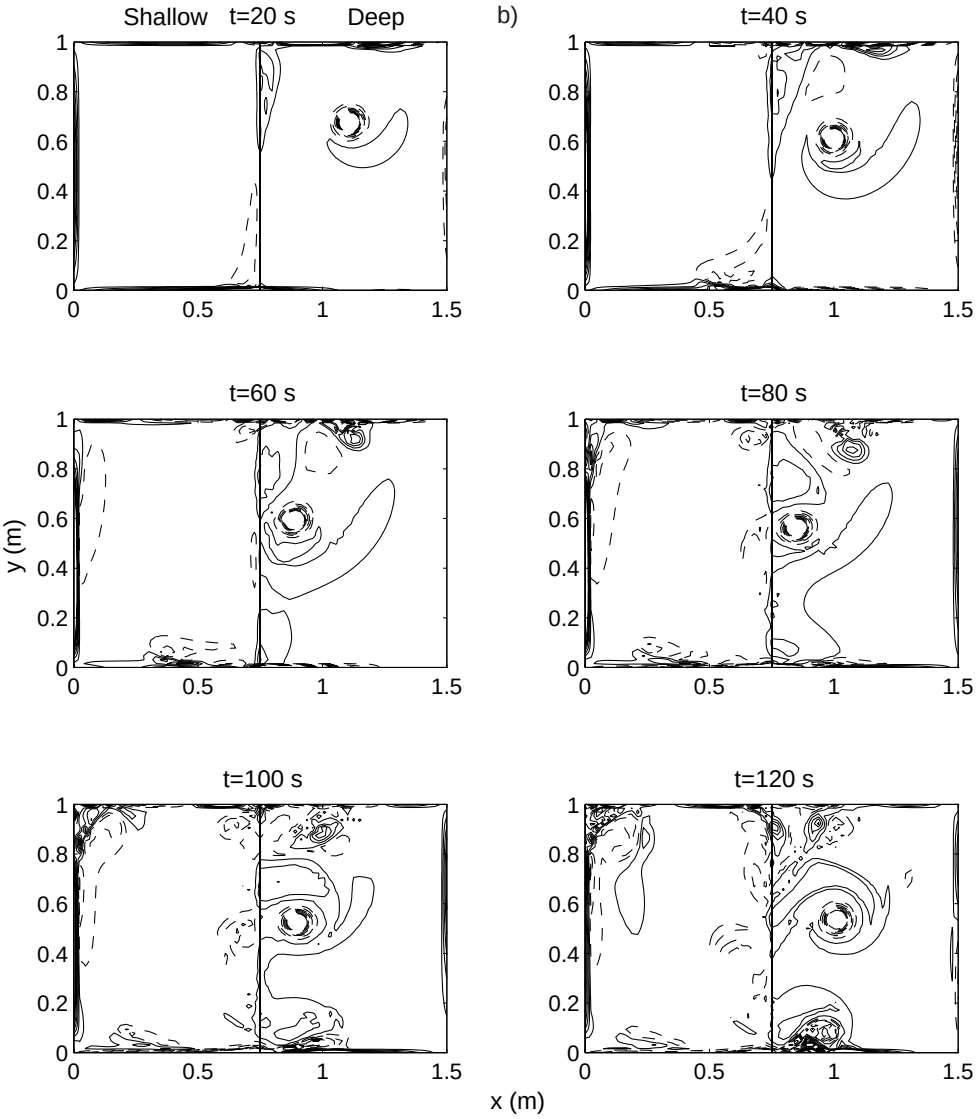

Fig. 8. – (*Continued.*) b) As in fig. 7b).

$$\omega^{-} = -f_0 \frac{\Delta H}{(H_0 + \Delta H)}, \tag{7}$$

where ω^{-} is estimated by conservation of potential vorticity on fluid columns crossing the step, *i.e.* from $f_0/(H_0 + \Delta H) = (\omega^{-} + f_0)/H_0$. The reflection is produced when ω^{-} is a significant fraction of ω^{+} (in absolute value). Under these considerations, it is not possible to determine precisely how significant should ω^{-} be in order to produce the vortex reflection. However, from (6) and (7) it can be established that the reflection effect will be enhanced by decreasing the initial vortex strength or by increasing the

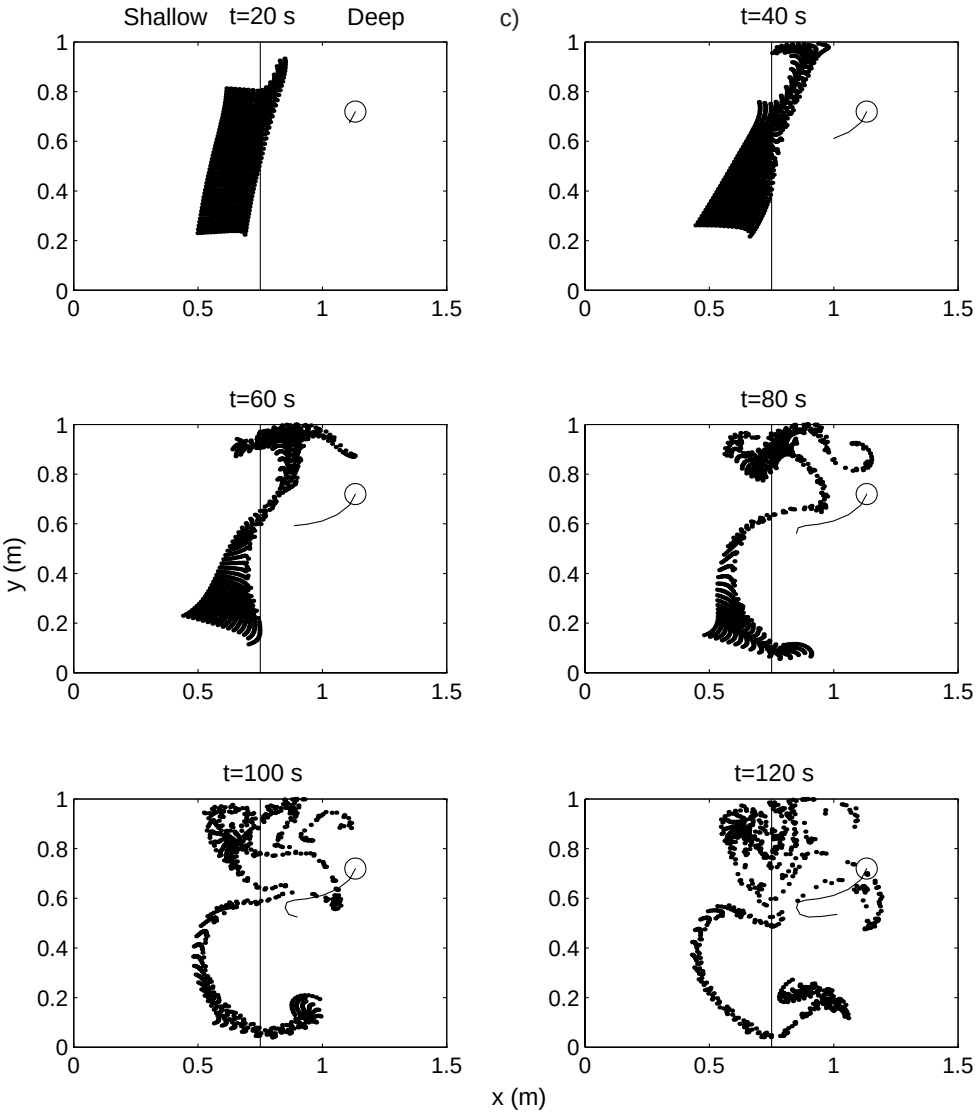

Fig. 8. – (*Continued.*) c) As in fig. 7c).

step height, because in both cases the negative half of the dipole will be increased compared with the positive half.

These assertions are confirmed by results of numerical simulations shown in fig. 9. Two different vortices ($\omega_0^{(1)} = 2.5\,\mathrm{s}^{-1}$ and $\omega_0^{(2)} = 1.25\,\mathrm{s}^{-1}$) approach two different step-down topographies. In all cases the vortex radius and the initial position are $R = 0.04$ m and $(x_0, y_0) = (1.10\,\mathrm{m},\ 0.25\,\mathrm{m})$, respectively. In the first plot, the vortices approach a step-down with $\Delta H = 0.04$ m. It is observed that both vortices are reflected from the step, but vortex (2) is reflected earlier than vortex (1). In other words, the reflection effect increases as the vortex is weaker. In the second plot, the vortices

approach a step-down with $\Delta H = 0.01$ m. In this case, vortex (1) is able to cross the step because the negative patch created from the interaction with the topography is not able to stop the vortex drift completely (not shown here). However, during some time the vortex moves northward along the step. On the other hand, vortex (2) (which is less intense) is still reflected from the step, although very weakly. Therefore the reflection effect decreases (or even does not take place) when the step height is reduced, as expected.

Using the same arguments for the case of an anticyclonic vortex approaching a step-up ($\omega_0 < 0$, $\Delta H < 0$), the peak vorticities of the dipolar structure formed during the vortex-step interaction are given by

$$\omega^+ = f_0 \frac{\Delta H}{(H_0 - \Delta H)}, \tag{8}$$

$$\omega^- = -\omega_0. \tag{9}$$

From these expressions, it is expected that the reflection of an anticyclone from a step-up will be stronger than the reflection of a cyclone from a step-down, since the topographically induced vorticity in the former case is larger (compare (7) and (8)). This can be observed in the vortex trajectories shown in figs. 7c and 8c. Note that when

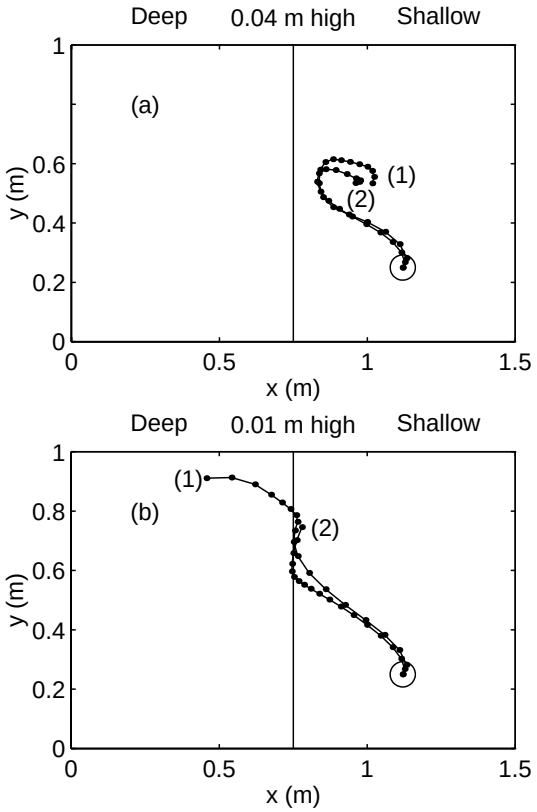

Fig. 9. – Numerical trajectories of two cyclonic vortices ($\omega_0^{(1)} = 2.5\ \mathrm{s}^{-1}$, $\omega_0^{(2)} = 1.25\ \mathrm{s}^{-1}$) approaching a step-down. (a) $\Delta H = 0.04$ m. (b) $\Delta H = 0.01$ m.

$|\Delta H|/H_0 \ll 1$, relations (7) and (8) tend to the same limit (in absolute value). It can be shown that, under this restriction, both cases are nearly symmetric about a zonal axis (see the appendix).

4. – Discussion

In this paper, the evolution of a barotropic vortex on a β-plane, approaching a step-like topography has been examined by means of laboratory experiments and numerical simulations. The initial situation was a cyclonic (anticyclonic) vortex, drifting to the northwest (southwest) on the β-plane, and approaching either a step-down or a step-up topography. The study is mainly focused on cases in which the depth-variation and the vortex circulation are both positive or negative, *i.e.* when $\omega_0 \Delta H > 0$. In these situations, cyclonic vortices cannot cross a step-down topography ($\omega_0 > 0$, $\Delta H > 0$), and anticyclonic vortices are not able to cross a step-up topography ($\omega_0 < 0$, $\Delta H < 0$). This behaviour has been termed "reflection". The other two possible cases ($\omega_0 \Delta H < 0$) lead to very different results, namely, the cyclonic (anticyclonic) vortex is able to cross a step-up (step-down) topography. When $|\Delta H|/H_0 \ll 1$, the two cases $\omega_0 \Delta H > 0$ are symmetric about a zonal axis, as well as the $\omega_0 \Delta H < 0$ situations.

The reflection of cyclonic vortices was observed in laboratory experiments, while the anticyclonic case was studied only by numerical simulations, due to the experimental difficulties to produce anticyclones in the laboratory. This dramatic effect on the vortex trajectory is due to the formation of an oppositely signed vorticity patch at the southern (northern) part of the cyclone (anticyclone) as the vortex reaches the step-down (up). This patch is formed from the fluid that the vortex has dragged from the west side of the tank. In the cyclonic case, the entrained fluid moves from deep into shallow parts of the tank, and therefore acquires negative relative vorticity as fluid columns are squeezed. As a result, this fluid forms together with the cyclone a dipolar structure moving away from the step. The experiments end when the vortex has been dissipated by lateral viscous effects (and bottom friction in the laboratory). Previous arguments do not apply for cyclonic (anticyclonic) vortices approaching a step-up (down) topography, since the entrained fluid from the western side will acquire relative vorticity having the same sign as the vortex. Therefore, the dipolar structure is not formed and the vortex is able to cross the step.

It was shown that the reflection effect will be enhanced either by decreasing the initial vortex strength (ω_0) or by increasing the step height (ΔH). This is because in both cases the topographically induced half of the dipole structure (created by the vortex-step interaction) will be increased compared with the vortex itself. In a similar way, the reflection effect is reduced by increasing the initial vortex strength or by decreasing the step height. It was also found that the reflection of an anticyclone from a step-up is stronger than the reflection of a cyclone from a step-down. Even though the numerical results support these assertions, these arguments are not conclusive, since they are based on the assumption that the vortex behaviour is determined by the peak vorticities of the dipolar structure. Additional work should be done to investigate the rather complex vorticity distributions around the vortex during the interaction with the step. Besides, the vortex decay by viscous effects should also be taken into account.

The β-effect plays a fundamental role in the experiments and simulations described above, since it induces the vortex motion toward the step. With regard to the vortex

reflection mechanism, it was found that the Rossby wave radiation generated by the vortex reinforces the strength of the topographically induced negative (positive) circulation patch, which pairs with the cyclone (anticyclone), thus contributing to stop the vortex. However, the influence of β on the vortex reflection mechanism is not fundamental. This was observed in numerical simulations (not shown here) of a cyclonic vortex near a step-down and setting $\beta = 0$. As before, the entrained fluid from the deep side (induced by the vortex) acquires negative relative vorticity and forms together with the cyclone a dipolar structure, which moves far from the step. Similar results have been found by McDonald and Dunn (personal communication) using contour dynamics simulations.

* * *

LZS gratefully acknowledges financial support from the Consejo Nacional de Ciencia y Tecnología (CONACYT, México) and from Eindhoven University of Technology (TUE).

APPENDIX

In this appendix it is shown that the vortex trajectories in the case of an anticyclone approaching a step-up ($\omega_0 < 0$, $\Delta H < 0$) and in the case of a cyclonic vortex approaching a step-down ($\omega_0 > 0$, $\Delta H > 0$) are symmetrical about an east-west axis. Analogously, the cases $\omega_0 \Delta H < 0$ are also symmetric about a zonal axis. These symmetries are illustrated by the calculated trajectories shown in fig. 10.

In most of the laboratory experiments and numerical simulations the total mean depth was much larger than the topographic variations. Writing the layer depth $h = H_0 + \Delta H$, and assuming $|\Delta H|/H_0 \ll 1$, eq. (4) can be written as

$$\frac{\partial}{\partial t}(\nabla^2 \psi) + J(\nabla^2 \psi + \eta, \psi) + \beta \frac{\partial \psi}{\partial x} = \nu \nabla^2 (\nabla^2 \psi), \tag{A.1}$$

where the stream function is related to the vorticity through a Poisson equation, and η is given by

$$\eta(x, y) = -f_0 \frac{\Delta H(x, y)}{H_0}. \tag{A.2}$$

In general, the topographic term, ΔH, may be a function of x and y. When only the β-plane is considered ($\eta = 0$) eq. (A.1) is invariant under the transformation

$$T_1 : \{\psi, y\} \to \{-\psi, -y\}.$$

This is a well-known symmetry about an east-west axis for vortices on a β-plane: when cyclones move northwestward, anticyclones would move southwestward (see, *e.g.*, Hopfinger and van Heijst, 1993). When topographic changes are considered ($\eta \neq 0$), this property no longer holds (in general) and the symmetry may be broken, depending on the topographic term. Indeed when $\eta(x, -y) = -\eta(x, y)$ (*i.e.* when η is an odd function of y) the zonal symmetry is conserved because the form of (A.1) remains the same. This could be the case of a linear bottom slope in the y direction, $\eta(x, y) = sy$ with constant s, which simulates the β-plane ($s \ll 1$ necessarily, in order to keep $|\Delta H|/H_0 \ll 1$).

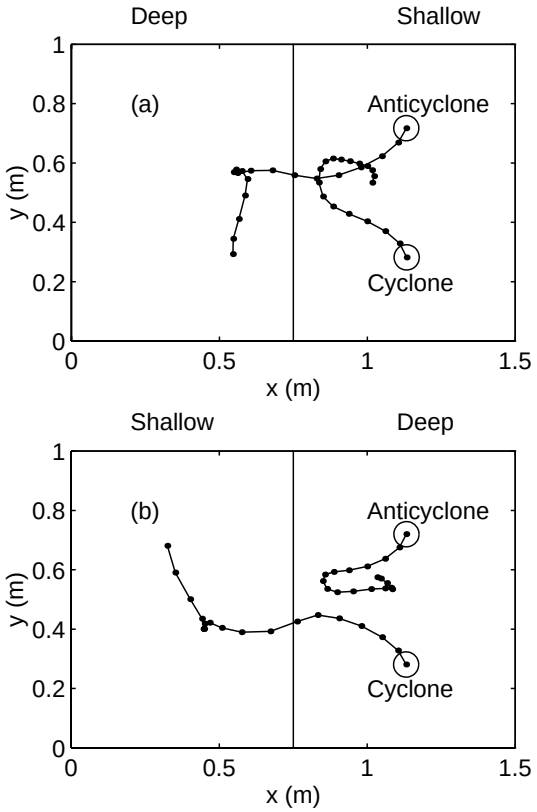

Fig. 10. – Numerical trajectories of cyclonic and anticyclonic vortices meeting (a) a step-down and (b) a step-up.

On the other hand, consider the transformation

$$T_2: \{\psi, y, \eta\} \to \{-\psi, -y, -\eta\}.$$

Equation (A.1) is invariant under T_2 when $-\eta(x, -y) = -\eta(x, y)$, that is when η is an even function of y. In particular, let the topographic term be only x-dependent, $\eta(x)$, as in the numerical experiments. For this case, the symmetry about a zonal axis remains. Thus, replacing cyclones for anticyclones and hills for valleys (assumed only x-dependent), the flow evolution will be symmetric about the east-west axis. In other words, there will be a zonal symmetry between the flow ψ over the topography η, and the oppositely signed flow $-\psi$ over the topography $-\eta$. It must be remarked that these considerations are only valid as long as the quasi-geostrophic approximation holds, *i.e.* when ($|\Delta H|/H_0 \ll 1$).

Figure 10 illustrates the symmetries already described between cases where the reflection is produced ($\omega_0 \Delta H > 0$) and between cases where the vortices cross the step ($\omega_0 \Delta H < 0$). The figure shows the vortex trajectories of the four possible situations calculated from numerical simulations. The initial vortex parameters were $\omega_0 = \pm 2.5\ \mathrm{s}^{-1}$, $R = 0.04$ m and the initial positions $(x_0, y_0) = (1.10\ \mathrm{m},\ 0.25\ \mathrm{m})$ for the cyclones, and $(x_0, y_0) = (1.10\ \mathrm{m},\ 0.75\ \mathrm{m})$ for anticyclones. The step height was $\Delta H = \pm 0.04$ m. Note that the symmetry about the zonal axis is not exact. The reason is that $|\Delta H|/H_0 \sim 1/5$, while the symmetry arguments only apply to the case $|\Delta H|/H_0 \ll 1$.

Note also that the zonal symmetry is broken in the laboratory experiments, where there is no β-effect, but a topographic β-effect provided by the bottom slope in y-direction. However, the numerical results (where a real β-effect and an x-dependent topography were considered) show that deviations from symmetry are expected to be small.

REFERENCES

Byrne D. A., Gordon A. L. and Haxby W. F., *Agulhas Eddies: a synoptic view using Geosat ERM data*, *J. Phys. Oceanogr.*, **25** (1995) 902-917.

Carnevale G. F., Kloosterziel R. C. and van Heijst G. J. F., *Propagation of barotropic vortices over topography in a rotating tank*, *J. Fluid Mech.*, **233** (1991) 119-139.

Dalziel S., *Digimage. Image Processing for Fluid Dynamics* (Cambridge Environmental Research Consultants Ltd.) 1992.

Dewar W. K. and Gailliard C., *The dynamics of barotropically dominated rings*, *J. Phys. Oceanogr.*, **24** (1994) 5-29.

Grimshaw R., Broutman D., He X. and Sun P., *Analytical and numerical study of a barotropic eddy on a topographic slope*, *J. Phys. Oceanogr.*, **24** (1994) 1587-1607.

Hopfinger E. J. and G. J. F. van Heijst, *Vortices in rotating fluids*, *Annu. Rev. Fluid Mech.*, **25** (1993) 241-289.

Kamenkovich V. M., Leonov Y. P., Nechaev D. A., Byrne D. A. and Gordon A. L., *On the influence of bottom topography on the Agulhas Eddy*, *J. Phys. Oceanogr.*, **26** (1996) 892-912.

Kloosterziel R. C. and van Heijst G. J. F., *An experimental study of unstable barotropic vortices in a rotating fluid*, *J. Fluid Mech.*, **223** (1991) 1-24.

Orlandi P., *Vortex dipole rebound from a wall*, *Phys. Fluids A*, **2** (1990) 1429-1436.

van Geffen J. H. G. M., *NS-evol*, Internal report R-1466-D, Department of Physics, Fluid Dynamics Laboratory, Eindhoven University of Technology, The Netherlands (1998).

van Heijst G. J. F., *Topography effects on vortices in a rotating fluid*, *Meccanica*, **29** (1994) 431-451.

Zavala Sansón L. and van Heijst G. J. F., *Interaction of barotropic vortices with coastal topography: Laboratory experiments and numerical simulations*, to be published in *J. Phys. Oceanogr.*, 1999.